Diabetologia (2010) 53:2579–2588
DOI 10.1007/s00125-010-1912-8

ARTICLE

mRNA expression analysis of cell cycle genes in islets of pregnant mice

A. Schraenen · G. de Faudeur · L. Thorrez · K. Lemaire · G. Van Wichelen · M. Granvik · L. Van Lommel · P. in't Veld · F. Schuit

Received: 19 May 2010 / Accepted: 17 August 2010 / Published online: 1 October 2010

Abstract
Aims/hypothesis Pregnancy requires an increase in the functional beta cell mass to match metabolic needs for insulin. To understand this adaptation at the molecular level, we undertook a time course analysis of mRNA expression in mice.
Methods Total RNA extracted from C57Bl6/J mouse islets every 3 days during pregnancy was hybridised on commercially available expression arrays. Gene network analysis was performed and changes in functional clusters over time visualised. The function of putative novel cell cycle genes was assessed via silencing in replicating mouse insulinoma 6 (MIN6) cells.
Results Gene network analysis identified a large gene cluster associated with cell cycle control (67 genes, all upregulated by ≥1.5-fold, $p<0.001$). The number of upregulated cell cycle genes and the mRNA expression levels of individual genes peaked at pregnancy day (P)9.5. Filtering of poorly annotated genes with enhanced expression in islets at P9.5, and in MIN6 cells and thymus resulted in further studies with *G7e* (also known as *D17H6S56E-5*) and *Fignl1*. Gene knock-down experiments in MIN6 cells suggested that these genes are indeed involved in adequate cell cycle accomplishment.
Conclusions/interpretation A sharp peak of cell cycle-related mRNA expression in islets occurs around P9.5, after which beta cell replication is increased. As illustrated by the identification of *G7e* and *Fignl1* in islets of pregnant mice, further study of this distinct transcriptional peak should help to unravel the complex process of beta cell replication.

Keywords Beta cell · Cell cycle · *Fignl1* · *G7e* · Islets of Langerhans · Pregnancy · Replication

A. Schraenen and G. de Faudeur contributed equally to this work.

Electronic supplementary material The online version of this article (doi:10.1007/s00125-010-1912-8) contains supplementary material, which is available to authorised users.

A. Schraenen · G. de Faudeur · L. Thorrez · K. Lemaire · M. Granvik · L. Van Lommel · F. Schuit (✉)
Gene Expression Unit, Department of Molecular Cell Biology, Katholieke Universiteit Leuven,
Herestraat 49, mailbox 901,
3000 Leuven, Belgium
e-mail: frans.schuit@med.kuleuven.be

L. Thorrez
Department of Electrical Engineering, ESAT-SCD, Katholieke Universiteit Leuven,
Leuven, Belgium

L. Thorrez · F. Schuit
Center for Computational Systems Biology, SymBioSys, Katholieke Universiteit Leuven,
Leuven, Belgium

G. Van Wichelen · P. in't Veld
Department of Pathology, Vrije Universiteit Brussel,
Brussels, Belgium

Abbreviations

CFSE	Carboxyfluorescein succinimidyl ester
MIN6	Mouse insulinoma 6
Mki67	Antigen identified by monoclonal antibody Ki67
P	Pregnancy day
siRNA	Small interfering RNA

Introduction

An important objective in islet research is to understand how functional beta cell mass is controlled [1–3]. Powerful

mechanisms tightly control the rate of insulin production and release to meet metabolic demands, since the latter is known to fluctuate during healthy life [4, 5] and to increase in conditions associated with insulin resistance [6]. Because excess and shortage of insulin are harmful to the organism, the regulation of beta cell proliferation has to be very precise. As in other cell types, control of the cell cycle in beta cells hinges on the transition between G0 and G1, and involves interactions between cyclin D isoforms, cyclin-dependent kinases and cyclin-dependent kinase inhibitors [2, 3]. Knockout and transgenic mouse models of these genes have inadequate beta cell mass phenotypes, protecting or predisposing to spontaneous or environmentally induced diabetes [2, 3, 7]. Recent molecular studies have led to a better insight into how cell cycle is regulated in beta cells [2, 3, 8]. For instance, the well-known declining potential for beta cell replication with advancing age is associated with increased cyclin-dependent kinase inhibitor 2A activity caused by loss of *Bmi1* expression [9]. An increased metabolic insulin demand together with a moderate degree of insulin resistance during pregnancy drives functional beta cell mass expansion [10]. The latter occurs via a gain of function of pre-existing beta cells [11] and enhanced beta cell replication [12, 13]. Prolactin receptors are known to be essential for such adaptation [11, 14, 15]; however, knowledge of the transcriptional response they trigger is still fragmentary. In addition, recent studies reported a role for Menin 1 [16], a tumour suppressor associated with multiple endocrine neoplasia type 1 [17], and for the transcription factor forkhead box M1 [18–21]. However, their relationship with cell cycle genes is still incompletely understood. To better understand beta cell replication, genome-wide mRNA expression analysis in islets from pregnant female animals has been used to screen for novel mechanisms [22]. We undertook a time course analysis of the transcriptional changes occurring in mouse pancreatic islets of Langerhans during pregnancy, isolating islets every 3 days of pregnancy. This detected a thus far unrecognised peak of cell cycle related gene activity on pregnancy day (P)9.5, which is just before mid-term.

Methods

Islet isolation All experiments with laboratory animals were approved by the committee for animal welfare at the Katholieke Universiteit Leuven, Belgium. Islets of Langerhans from female C57Bl6/J mice (Janvier, Le Genest-saint-Isle, France) were collagenase isolated as previously described [23]. Other tissues were dissected from 10- to 12-week-old male C57Bl6/J mice (Janvier). Tissues were rinsed in PBS, frozen in liquid nitrogen and stored at −80°C.

Cell culture Mouse insulinoma 6 (MIN6) cells were cultured in DMEM (Invitrogen, Carlsbad, CA, USA) with 25 mmol/l glucose equilibrated with 5% CO_2 and 95% air at 37°C. The medium was supplemented with 15% (vol./vol.) decomplemented fetal calf serum (Invitrogen, Paisley, UK), 70 μmol/l β-mercaptoethanol, 4 mmol/l glutamax, 50 U/ml penicillin and 50 μg/ml streptomycin. MIN6 cells were used between passages 20 and 30.

mRNA expression analysis via microarray Total RNA from mouse islets and MIN6 cells was extracted using a kit (Absolutely RNA microprep; Stratagene, La Jolla, CA, USA) according to the manufacturer's protocol. Total RNA was extracted from the other tissues as described previously [24]. The total RNA quantity and quality was determined using a spectrophotometer (ND-1000; NanoDrop Technologies, Wilmington, DE, USA) and a bioanalyser (2100; Agilent, Waldbronn, Germany), respectively.

The MOE430_2.0 arrays (Affymetrix, Santa Clara, CA, USA) were used as previously described on samples from P15.5 and non-pregnant females (n=4–5) [24]. To analyse the time series of pregnancy, 100 ng islet total RNA (n=4 for each time point except P3.5 [n=3]) was used to hybridise the arrays (MoGene_1.0_ST; Affymetrix) according to the manufacturer's manual 701880Rev4, as described previously [23].

Data analysis To identify differentially expressed genes between islets from non-pregnant and P15.5 mice with the MOE430_2.0 and MoGene_1.0_ST arrays (p<0.001), the probe sets of both platforms, unambiguously annotating the same gene, were analysed, resulting in an expression dataset of 17,337 genes. Differentially expressed genes in the time course analysis were identified on the basis of a fold change of ≥1.5 and p<0.001 at least at one of the pregnancy time points as compared with non-pregnant mice. The 415 differentially expressed genes were assigned by Gene Ontology (http://www.geneontology.org/, accessed April 2010) and consultation of the literature to cellular processes. A network of these genes was built based on multiple data sources obtained from String 8.0 [25], with an edge confidence score of >0.15. The network thus created was visualised in Cytoscape 2.6.1 (http://www.cytoscape.org/, accessed April 2010). Only the genes belonging to one of the five largest functional groups and having at least one connection with another gene in the same group were selected for visualisation, yielding a network of 130 genes. See also Electronic supplementary material (ESM) methods for heatmap and public microarray datasets analysis.

Quantitative RT-PCR After cDNA synthesis (RevertAid H Minus Reverse Transcriptase kit; Fermentas, St Leon-Rot, Germany), quantitative RT-PCR (Absolute QPCR mix;

Abgene Thermo Fisher Scientific, Waltham, MA, USA) was performed on a Rotorgene (Corbett Research, Mortlake, NSW, Australia) to determine mRNA expression of different genes (normalisation to RNA polymerase alpha II, *Polr2a*). For primers and probes, see ESM Tables 1 and 2.

Quantification of relative beta cell proliferation Pancreases were dissected from non-pregnant and pregnant female mice (n=3 for each time point except P6.5 [n=2] and non-pregnant [n=4]) and fixed in 4% (wt/vol.) paraformaldehyde. Next, paraffin sections were made and stained for antigen identified by monoclonal antibody Ki-67 (Mki67) and insulin using guinea pig anti-insulin (a gift from C. F. H. van Schravendijk, Diabetes Research Center, Vrije Universiteit Brussel, Brussels, Belgium) and rabbit anti-Mki67 (Acris Antibodies, Hiddenhausen, Germany) [26]. Binding of primary antibodies was detected with biotinylated anti-guinea pig and anti-rabbit Ig in combination with streptavidin horseradish peroxidase and alkaline phosphatase complex; diaminobenzidine and fuchsin-plus were used as substrates (all reagents from Dako, Glostrup, Denmark). Quantification of MKi67-insulin double positive cells was performed at ×400 magnification by two independent observers. A minimum of 1,000 cells per animal were evaluated.

RNA interference The small interfering RNAs (siRNAs) used in the study are listed in ESM Table 3. MIN6 cells loaded or not with the carboxyfluorescein succinimidyl ester (CFSE) according to the manufacturer's protocol (Cell Trace CFSE Cell Proliferation Kit; Invitrogen, Paisley, UK) were seeded in a 24-well plate and incubated for 24 h. For transfection, siRNA and DharmaFECT1 (ThermoFisher Scientific) were diluted separately in OptiMEM medium and incubated at room temperature for 5 min. Next, lipid–siRNA complexes were formed at room temperature for 20 min (1 μl DharmaFECT1, 20 pmol/l Fignl1 or 100 pmol/l siRNA [non-target, Dlk1, Kif11 and G7e]). The complexes were diluted and added to the cells for overnight transfection. Afterwards, cells were cultured for 24 to 48 h before mRNA extraction.

Analysis of proliferation and cell death On the 6th day after siRNA transfection, trypsinised CFSE-loaded MIN6 cells were resuspended in PBS containing 2 μg/ml propidium iodide to avoid contamination due to cell fragments or apoptotic cells. The fluorescence intensity of the cells was measured by flow cytometry. To determine the effect of silencing on the number of cells after culture, we took advantage of the time required to acquire a constant number of cells with the flow cytometer (Epix XL; Beckman-Coulter, Miami, FL, USA). From this time, the cell concentration of each sample could be deduced as $C_x=N/T_x$ (N being the fixed number of cells acquired, while T_x is the time necessary for cell acquisition from sample x). The percentage of MIN6 cells retrieved was calculated as $P=(C_x/C_{NT})\times 100$ (where C_x is the concentration of cells retrieved in sample x, while C_{NT} is the concentration of control MIN6 cells transfected with a non-target siRNA).

The proportion of apoptotic plus necrotic MIN6 cells was determined 48 h after siRNA transfection by their fluorescence intensity after staining with 2 μg/ml propidium iodide (dissolved in PBS) for 30 min at 4°C.

Results

Pancreatic islet mRNA expression of cell cycle genes peaks at day 9.5 of pregnancy To better understand the transcriptional response in islets of Langerhans during pregnancy, we assessed mRNA signals of islets ex vivo using MoGene_1.0_ST arrays. Since the time kinetics of changes in functional beta cell mass are not well characterised, we sampled islets every 3 days of pregnancy in the mouse, i.e. at P3.5, P6.5, P9.5, P12.5, P15.5 and P18.5, as well as 10 days postpartum, and compared their mRNA expression levels with those of non-pregnant age-matched controls. We found 415 differentially expressed genes defined by a fold change of ≥1.5 (up or down) and $p<0.001$ for at least one time point of pregnancy/lactation vs non-pregnant controls. These differentially expressed genes were mapped to their main functional process, while interactions were extracted from multiple data sources using String 8.0 [25]. Next, we performed a network analysis of the encoded proteins. Figure 1 visualises the five largest functional categories related to the differentially expressed genes during the time course of pregnancy. Almost all genes in the network were upregulated (95%). In this representation, the largest functional category (more than 50% of all the characterised and differentially expressed genes) encoded proteins involved in cell cycle. Remarkably, the expression of every gene in this cluster was upregulated at P9.5 (Fig. 1), while before and after this time point fewer cell cycle genes were differentially expressed (ESM Fig. 1). This functional cluster was not exclusively composed of positive cell cycle regulators, but also contained one inhibitor, *Cdkn2c*, which is a member of INK4a/ARF family and peaked at the same time point (ESM Fig. 2). In contrast, genes linked to other functional clusters (metabolism, signal transduction, cell growth and differentiation, and protein synthesis) did not exhibit a similar peak at P9.5, but were also altered at later time points, even at 10 days postpartum (ESM Fig. 1). In addition, we also found that the individual expression levels of all cell cycle genes in Fig. 1 peaked at P9.5 as illustrated in the heatmap representation (ESM Fig. 3). To further illustrate this point, we focused on three well characterised

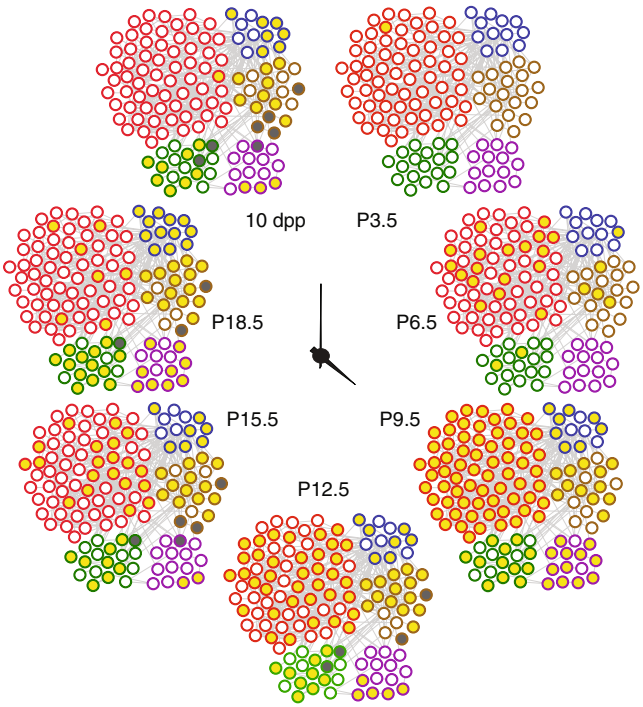

Fig. 1 Pregnancy-induced changes in islet mRNA expression. Network analysis, using String 8.0 and Cytoscape 2.6.1, of 130 genes with expert-assigned gene ontology that were found to be differentially expressed during one time point of pregnancy (P3.5, P6.5, P9.5, P12.5, P15.5, P18.5) or lactation (10 days postpartum [10 dpp]) as compared with non-pregnant control islets. Differentially expressed genes (fold change vs non-pregnant ≥1.5, $p<0.001$) with known function were clustered according to function. Representation is limited to genes that had at least one connection with another gene in the same group. The five largest functional categories in this figure are indicated by coloured circle outlines as follows: cell cycle (red), metabolism (green), signal transduction (brown), protein synthesis, modification and folding (purple), and beta cell growth and differentiation (blue). Circle shading indicates: yellow, gene upregulated; dark grey, gene downregulated ≥1.5 and $p<0.001$. Data analysis was performed as described in the Methods. Symbols of individual genes are listed for each cluster in ESM Fig. 3

cell cycle genes (*Mki67* [7], cyclin A2 [*Ccna2*] and topoisomerase 2-alpha [*Top2a*]), mRNA expression profiles of which were tightly correlated ($R>0.95$; $p<0.0001$), both at the level of expression in tissues that widely differ in number of proliferating cells (ESM Fig. 4a), and at the level of islets at different time points of pregnancy (ESM Fig. 4b). Together, we observed a clear time-dependent induction of cell cycle genes in islets from pregnant mice with a distinct maximum of mRNA expression centred at P9.5.

Islet beta cell proliferation peaks between the 2nd and 3rd week of mouse pregnancy The maximal transcriptional activity of cell cycle genes observed at P9.5 occurred 3 to 6 days before the peak of effective mouse beta cell proliferation during pregnancy as described in literature [12]. To better understand this difference, we confirmed by quantitative RT-PCR analysis the time course of *Mki67* mRNA expression in islets during pregnancy (Fig. 2a). In parallel, we quantified Mki67/insulin immunoreactive cells in pancreatic sections at the same time points (Fig. 2b, c). In control islets, less than 3% of beta cells were proliferating. This number doubled at P9.5 ($p<0.001$), but a further rise in proliferating beta cells (~8–9%) was achieved between P12.5 and P15.5. After this peak, the amount of proliferating beta cells returned to baseline by P18.5 and became significantly lower than baseline postpartum. In contrast, *Mki67* mRNA was still upregulated at P18.5 and 10 days postpartum as compared with non-pregnant islets. These data indicate that the orchestrated short peak of transcriptional activity of cell cycle genes is followed by several days of beta cell replication. Moreover, the different time kinetics between *Mki67* mRNA and protein in islets indicates a time-dependent translational control for this protein.

Two putative new cell cycle genes with highest mRNA expression in islets isolated on P9.5 A limitation of the network analysis used (Fig. 1) is that poorly annotated genes with uncharacterised function were excluded. Since some of these genes showed the same expression profile as the well characterised genes of the cell cycle cluster, including the distinct peak of transcription at P9.5, it is conceivable that such genes could play a role in cell cycle control of replicating beta cells during pregnancy. We therefore re-analysed from the set of 415 differentially expressed genes during pregnancy the 267 genes that were significantly upregulated on P9.5 (fold change ≥1.5, $p<0.001$). To enrich this group with proliferation-related genes, we next selected transcripts that were at least tenfold more abundant in thymus (269 genes from the whole array) and at least fivefold more abundant in the proliferating mouse beta cell line MIN6 (182 genes from the whole array) than in non-pregnant islets (Fig. 3a). Both conditions were chosen because of their enrichment of proliferating cells. Via this strategy 41 genes (including *Mki67*, *Top2a* and *Ccna2*) were seen to be represented in the overlapping area of the Venn diagram (Fig. 3a) and were listed according to gene symbol in Fig. 3b. According to Gene Ontology annotation, 35 of these 41 genes were classified as cell cycle genes, of which 30 were also selected as genes of the cell cycle category in our first analysis in ESM Fig. 1. In contrast, *Arhgap11a* was the sole exception assigned to the signal transduction category by Gene Ontology analysis. Among the remaining five genes, three were not yet correctly classified in Gene Ontology, but the literature indicated that these were indeed cell cycle genes, namely *C330027C09Rik, C79407* and *2810417H13Rik*, which (or human homolog) are now respectively called

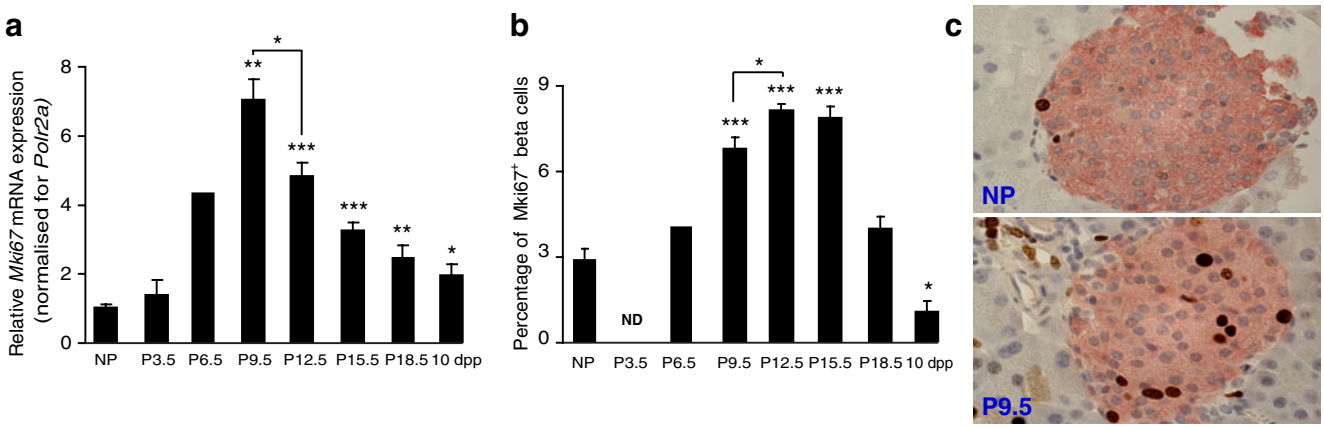

Fig. 2 Islet *Mki67* mRNA expression and protein level during pregnancy. **a** *Mki67* mRNA expression, measured via quantitative RT-PCR, reached a peak at P9.5. Data represent mean±SEM of three to four independent experiments (except P6.5, $n=2$) and are presented as fold change over the non-pregnant condition. **b** Beta cell proliferation (expressed as % of insulin-positive cells) was assessed by Mki67 immunostaining of pancreatic sections. This percentage peaked at P12.5, i.e. 3 days after the peak mRNA expression level. Data represent mean±SEM, three animals per time point (except non-pregnant, $n=4$ and P6.5, $n=2$). ND, not determined. *$p<0.05$, **$p<0.01$ and ***$p<0.001$ for difference between non-pregnant and pregnant or postpartum conditions. **c** Representative images of Mki67 immunoreactivity (brown) in insulin-positive beta cells (pink) of islets in pancreatic sections from non-pregnant (NP) and P9.5 mice

Cip2a, *Mis18bp* and *p15(PAF)* [27, 28]. *Fignl1* had already been linked to the cell cycle, but up to now with discrepant effects [29, 30]. The last gene called, *G7e*, also known as *D17H6S56E-5*, was essentially uncharacterised, although located in a tumour susceptibility locus [31, 32]. Expression of *Fignl1* and *G7e* was strongly correlated with essential cell cycle genes in public human and mouse microarray databases, analysed via Multi Experiment Matrix: MEM [33] (ESM Tables 4 and 5). *Fignl1* was also overexpressed in different human cancers (ESM Table 6) [34], whereas *G7e* could not be analysed with the human arrays, as it is rodent-specific. Therefore, we chose the last two genes, *G7e* and *Fignl1*, to study their contribution to cell cycle in proliferating MIN6 cells.

Effect of G7e and Fignl1 silencing on proliferation of MIN6 cells The idea that *G7e* and *Fignl1* are related to the cell cycle is supported by the following observations. First, mRNA expression of *G7e* and *Fignl1*, as well as of *Arhgap11a*, *Mis18bp* and *2810417H13Rik* correlated well with *Mki67* mRNA expression in the individual islet preparations examined during pregnancy, with the highest expression level occurring in P9.5 islet samples (Fig. 4). These data were confirmed by quantitative RT-PCR, as well as for *Top2a* and *Mis18bp* (Fig. 2a, ESM Fig. 5). To further characterise the function of these putative new cell cycle genes, we silenced their expression by RNA interference (siRNA) in proliferating MIN6 cells. As a positive control, we silenced *Kif11*, a known cell cycle gene, whereas as a negative control we used siRNA targeting *Dlk1*. For all four tested genes, 60 to 90% silencing was achieved (Fig. 5a). On the basis of a flow cytometric analysis, we found no influence on proliferation when MIN6 cells were transfected with siRNA directed against *Dlk1* since the same number of cells (94±10%, $n=3$) was obtained as compared with non-target control, which was set to 100% for each experiment (Fig. 5b). In contrast, silencing of *Kif11* resulted in a significant reduction (43±7%, $p<0.001$, $n=5$) as compared with non-target. In addition, silencing of *G7e* or *Fignl1* also led to a significant reduction of MIN6 cells (63±2%, $p<0.001$ and 58±8%, $p<0.001$ respectively). The reduced number of cells could be the consequence of impaired cell cycle entry (G0-G1 transition), cell-cycle progression (G1-M) or enhanced cell death due to cell cycle checkpoint alert. To distinguish between these possibilities, we first tested the effect of siRNA on entry in the S-phase by 5-ethynyl-2′-deoxyuridine incorporation. As shown in ESM Fig. 6, none of the silenced genes was able to change the rate of cells that entered the S-phase. Next, the reduced ability to proliferate was tested via the loss of CFSE fluorescence of coloured cells (Fig. 6), since the intensity of the fluorescent dye is diluted two times at each round of cell division, thereby allowing us to follow individual cell division history [35]. The percentage of ‘CFSE-high’ cells (i.e., cells that are replicating slowly) (Fig. 6) was measured 6 days after transfecting MIN6 cells with non-target siRNA or siRNA directed against *Kif11*, *G7e* or *Fignl1*. The percentage of cells replicating slowly in non-treated controls (20±2%) was significantly ($p=0.01$) lower than in the condition of *Kif11* knockdown (31±4%). Likewise, knockdown of *G7e* resulted in a significantly ($p=0.005$) greater number of slowly replicating cells (32±2%). In contrast, no increment in slowly replicating cells was found after knockdown of *Fignl1* (21±1%; $p=0.64$).

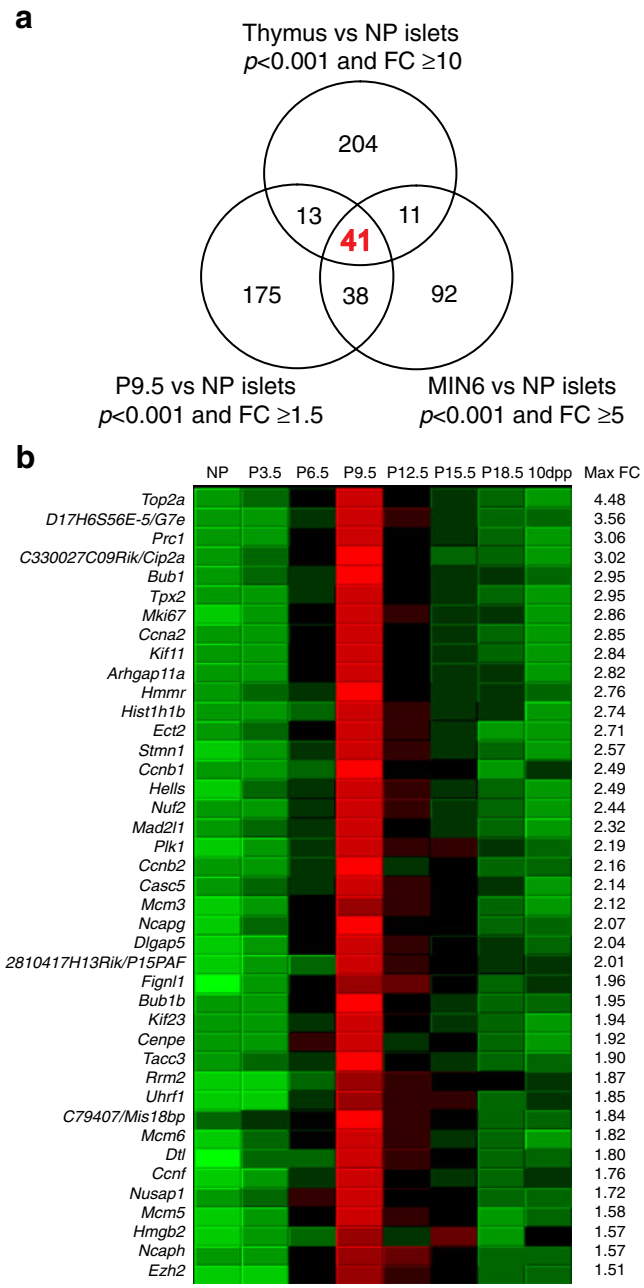

Fig. 3 Identification of novel cell cycle genes involved in beta cell proliferation during pregnancy. **a** Microarray analysis was performed on thymus, MIN6 cells and islets of Langerhans isolated from non-pregnant and P9.5 mice. For 41 putative cell cycle genes (overlapping area between three circles) the three following criteria were met: (1) differential expression (fold change ≥1.5, $p<0.001$) in islets of P9.5 vs non-pregnant mice; (2) increased expression in MIN6 cells (fold change ≥5, $p<0.001$) vs islets of non-pregnant mice; and (3) increased expression in thymus as compared with control islets (fold change ≥10, $p<0.001$). **b** The 41 putative cell cycle genes, listed according to the associated Entrez Gene ID and ranked on basis of their expression induction in islets on P9.5 as compared with non-pregnant control (maximum fold change). Two of these genes, *G7e* and *Fignl1*, are poorly characterised and were chosen for further studies. In addition, *2810417H13Rik*, *C330027C09Rik* and *Mis18bp* have emerged in the recent literature as cell cycle genes, but were not listed in Gene Ontology annotation [27, 39, 40]. *Arhgap11a* was classified as involved in cell signalling

In a third assay, we stained MIN6 cells with propidium iodide and counted the number of apoptotic plus necrotic cells. Silencing of *Kif11* enhanced the number of dead MIN6 cells with an increase of 23±11% as compared with non-target controls ($p=0.015$, $n=3$) and an even stronger effect seen when *Fignl1* was silenced (39±14% dead cells above basal, $p=0.003$, $n=3$). In contrast, silencing of *G7e* did not affect the rate of MIN6 cell death. Altogether, our data support the idea that *G7e* and *Fignl1* should be considered as genes that contribute to the cell cycle of beta cells; *Fignl1* also seems to control cell survival.

Discussion

To better understand the complex mechanism of beta cell mass regulation during pregnancy, we undertook a genome-wide mRNA analysis of mouse islets ex vivo, conducted on every third day of pregnancy. This approach is different from that used in the study by Rieck et al., which focused on the last third of gestation when the effective functional beta cell mass expands most dramatically [22]. With this approach, we were able to reconstitute a time course of mRNA changes related to the cell cycle and observed a sharp peak at an unexpected early time point, namely P9.5, during which a large cluster of genes related to the cell cycle was upregulated. Most of these genes encode cell cycle activators. However, *Cdkn2c*, a member of the INK4a/ARF family of inhibitors, also peaked at P9.5. This could mean that, in parallel to providing positive regulators of cell division, beta cells are also prepared to slow down the cell cycle. Regulation of cell cycle genes can occur at other levels than mRNA expression, e.g. protein translation, protein degradation, phosphorylation or cellular localisation [36, 37]. Thus, a possible scenario is that mRNA steps preparing to slow cell division are made at P9.5, whereas the actual slowing process, based on phosphorylation and localisation of the protein, occurs later in pregnancy.

Importantly, a temporary wave of cell cycle gene mRNA expression, measured as a sharp peak of cell cycle gene activity at mid-gestation in mouse islets, was followed by a period of about 1 week of enhanced beta cell proliferation. The mechanism supporting this sustained beta cell proliferation during pregnancy is not known and needs further investigation. While transcriptional activity seems to be synchronised, the biological response of beta cells could be heterogeneous. One possibility is that a repressor of mRNA translation, for instance one or several micro-RNAs, has to be removed before cell division can occur. Another possibility is that the actual progress of beta cell replication needs, in addition to cell-cycle control in other cell types, a second signal for growth, which comes at a later time point.

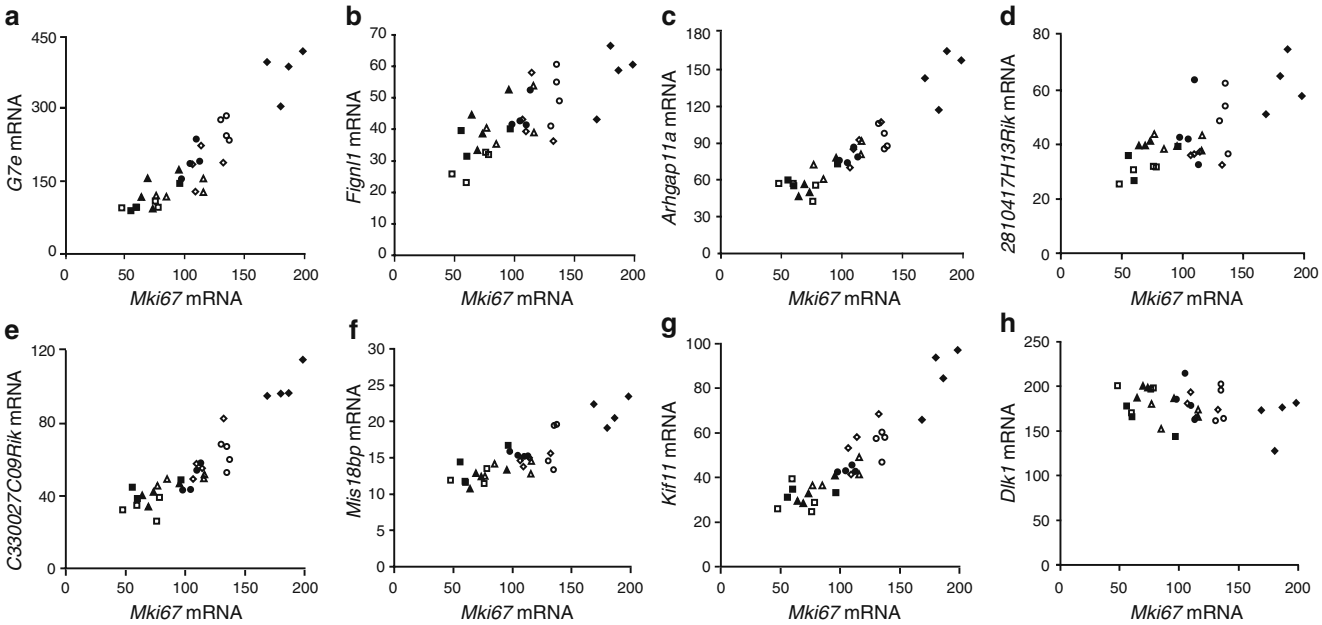

Fig. 4 Correlation between putative novel cell cycle gene expression and abundance of *Mki67* mRNA in mouse islets. Six genes from the set of 41 (see Fig. 3) are not linked to the cell cycle according to current Gene Ontology annotation. Microarray analysis showed that expression of each of these six genes in islets from pregnant mice correlated with the prototypic cell cycle marker *Mki67* during pregnancy. Graph representing the transcriptional correlations during pregnancy of *Mki67* with (**a**) *G7e* (r=0.93, p<0.0001), (**b**) *Fignl1* (r=0.75, p<0.0001), (**c**) *Arhgap11a* (r=0.93, p<0.0001), (**d**) *2810417H13Rik* (r=0.74, p<0.0001), (**e**) *C330027C09Rik* (r=0.93, p<0.0001), (**f**) *Mis18bp* (r=0.86, p< 0.0001), (**g**) *Kif11* (positive control; r=0.93, p<0.0001) or (**h**) *Dlk1* (negative control; r=0.30, p<0.10). White squares, non-pregnant; black squares, P3.5; white rhombuses, P6.5; black rhombuses, P9.5; white circles, P12.5; black circles, P15.5; black triangles, P18.5; white triangles, 10 days postpartum. mRNA expression of these uncharacterised genes significantly correlated (Pearson r correlation coefficient and p<0.0001) with *Mki67* mRNA expression in islets during pregnancy

In this context it is interesting that well-known genes for beta cell growth such as *Akt* (also known as *Akt1*) peaked during the last week of pregnancy in our analysis.

By focussing on the time-dependent expression of cell cycle genes at the peak time point of P9.5 in islets during pregnancy, we were able to screen for novel players in the cell cycle. We generated a list of 41 genes, of which 35 are well characterised cell cycle genes according to current Gene Ontology annotation. *Arhgap11a* is linked, according to its Gene Ontology annotation, to signal transduction, not cell cycle, possibly indicating that the protein it encodes could be involved in the signal transduction initiating the cell cycle or assisting in progression through G1/S transition as suggested in literature [38]. It will be interesting to unravel the signalling pathway in which Rho GTPase activating protein 11A is involved. Our mRNA analysis identified several receptors (*Insrr*, *P2ry1* and *Ptprd*) with expression peaking before P9.5, suggesting that the encoded proteins could be involved in early events preparing for the cell cycle.

The five remaining genes are still unclassified in Gene Ontology and are annotated as poorly characterised genes. The recent literature, however, connects several of these five genes to cell division. For *C330027C09Rik*, *C79407* and *2810417H13Rik,* a role in the cell cycle is clearly emerging [27, 39, 40], while *G7e* and *Fignl1* are less well characterised. Extensive mRNA expression data analysis from public databases (ESM Tables 4–6) links *G7e* and *Fignl1* to cell division, both in normal tissues and in tumours. Using a silencing approach in proliferating MIN6 cells, we showed that downregulation of *Fignl1* and *G7e* reduced cell proliferation. Results of *Fignl1* silencing were more complicated to interpret, as we mainly observed an effect on cell death, rather than on cell division; however, cell death could also be secondary, due to a detrimental cell cycle arrest [41, 42]. *Fignl1* is well conserved in eukaryotic cells (ESM Fig. 7a). The literature on fidgetin-like 1 (FIGNL1) in animal cell proliferation is conflicting. Thus in calvarial cells and osteoblast cell line MC3T3-E1, silencing of mRNA expression resulted in enhanced proliferation [30]. In contrast, in *Caenorhabditis elegans* [29] or mouse islets and MIN6 cells, *Fignl1* seems to have a positive effect on proliferation. Remarkably, the rodent-specific *G7e* (ESM Fig. 7b), located in the major histocompatibility complex class III, is homologous to the envelope protein of murine leukaemia virus and maps in a lung tumour susceptibility locus [31, 32]. The intriguing possibility therefore is that a virally transduced gene stably integrated in the mouse genome is expressed in a regulated manner in order to support cell division, but also controls susceptibility to tumour development.

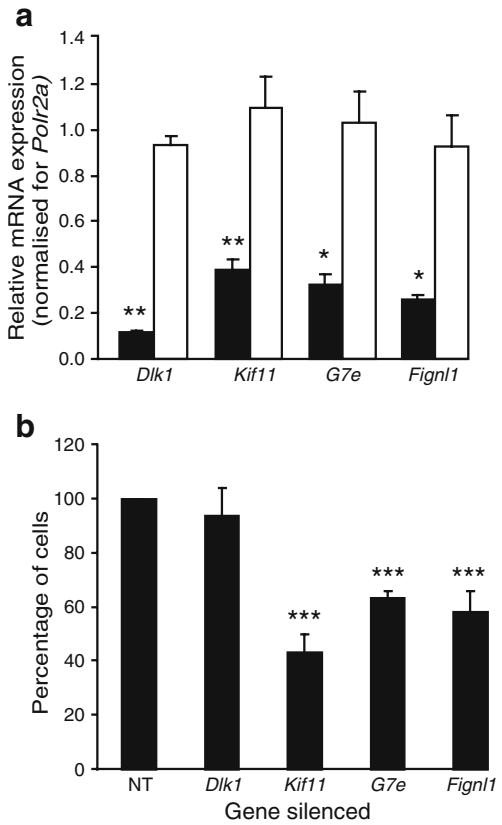

Fig. 5 Effect of *G7e* and *Fignl1* gene silencing on the number of cultured MIN6 cells. **a** mRNA expression levels after silencing (black bars) of *Dlk1* (negative control), *Kif11* (positive control), *G7e* and *Fignl1* or using a non-target siRNA (white bars); expression was determined by quantitative RT-PCR. Data are mean±SEM, $n \geq 3$, *$p<0.05$ and **$p<0.01$ **b** Relative MIN6 cell number counted by flow cytometry after silencing of *Dlk1*, *Kif11*, *G7e* and *Fignl1* as compared with MIN6 cells transfected with a non-target (NT) siRNA (set to 100% for each experiment). Data are mean±SEM, $n \geq 3$, ***$p<0.001$ for the *Z* test

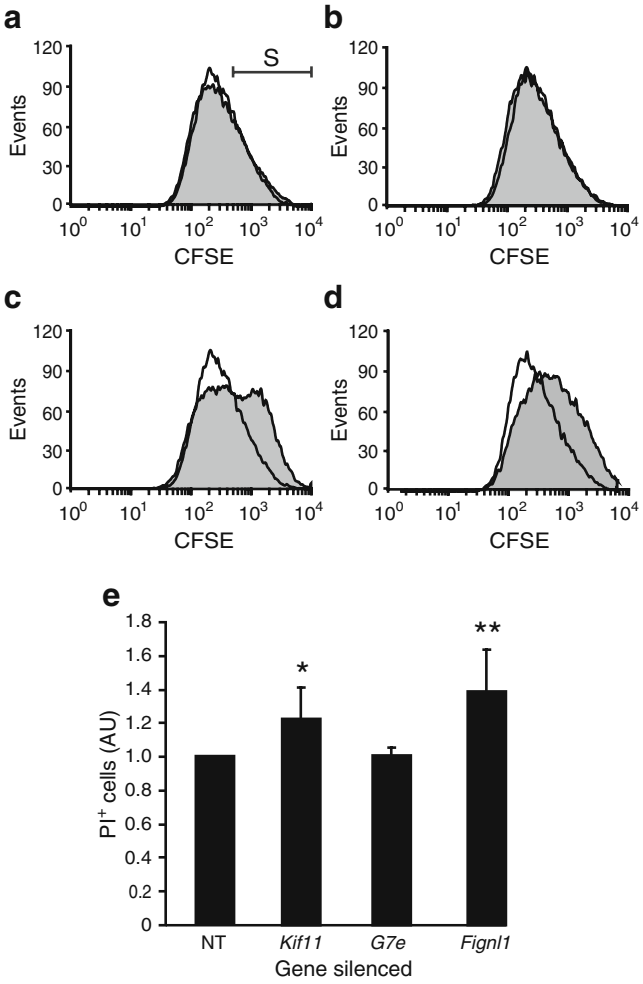

Fig. 6 Effect of *G7e* and *Fignl1* silencing on proliferation and cell death of MIN6 cells. MIN6 cells that were transfected (grey in histograms) with (**a**) a non-target siRNA (negative control), or siRNA directed against (**b**) *Fignl1*, (**c**) *Kif11* (positive control) or (**d**) *G7e* were loaded with the fluorescent dye CFSE and cultured for 6 days. The fluorescence intensity was measured by flow cytometry to evaluate the cell division history via dye dilution. Profiles obtained were compared with non-transfected control MIN6 cells (control, white in histograms). Data are representatives of at least three independent experiments. **e** MIN6 cells silenced for *Kif11, G7e* and *Fignl1* were stained with propidium iodide (PI) 48 h after transfection. The proportion of propidium iodide-positive cells was measured by flow cytometry and normalised to the non-target (NT) control. Values in arbitrary units (AU). Data are mean±SEM, $n=3$, *$p<0.05$ and **$p<0.01$ for difference by *Z* test from value 1 (non-target control)

Kinesin family member 11 is involved in the correct segregation of chromosomes [43–45] and was recently reported as a potential pharmacological target of anti-cancer drugs [46]. *Kif11* was one of the cell cycle genes identified in islets of pregnant mice with peak expression at P9.5; interestingly, single nucleotide polymorphisms around this gene are among the strongest genetic markers of type 2 diabetes in genome-wide association studies [47]. Therefore, the reduced cell proliferation obtained after mild *Kif11* silencing supports the idea that a genetic defect in human *KIF11* could predispose to type 2 diabetes via a beta cell mass defect.

For technical or other reasons, we will have failed to detect other genes that are important for beta cell proliferation. Indeed, *Foxm1* and *Men1* were not found to be differentially expressed in our screen (Fig. 1), yet they have been reported to regulate beta cell mass during pregnancy [16–21]. The cut-off levels used to screen for differentially expressed genes may be partly responsible. Indeed, *Foxm1* was significantly upregulated (fold change 1.6) on P9.5 (ESM Fig. 8a), but had only a *p* value of $p=0.03$, while we used $p=0.001$ as cut-off. On the other hand, we were not able to detect any decrease in *Men1* expression during pregnancy, neither by microarray (ESM Fig. 8b) nor by quantitative RT-PCR (results not shown). Therefore the use of more relaxed criteria could well have retained more new putative cell cycle genes. In spite of these limitations,

genes found to be differentially expressed on P15.5 are consistent with the recent report by Rieck et al. (ESM Table 7) [22]. In addition, tryptophan hydroxylase-1 (a key enzyme of serotonin biosynthesis) peaks at that time period. The companion paper to this manuscript, where we investigated pregnancy-induced serotonin production in islets, features data that do not support a role for islet *Tph1* expression in beta cell proliferation during pregnancy [48].

The last issue to be discussed is whether or not the orchestrated peak in cell cycle gene mRNA expression at mid-pregnancy in mouse islets is relevant for changes in beta cell mass in human pregnancies. Pioneering studies conducted three decades ago by Van Assche and colleagues indicated that beta cells of pregnant women can proliferate so that pancreatic beta cell mass increases >twofold during pregnancy [49]. Conversely, Butler and colleagues recently reported [50] a more modest 1.4-fold increase in pancreatic beta cell area, attributing this to the appearance of single or small beta cell clusters, rather than to beta cell proliferation or islet hypertrophy. The differences between these two studies may be due to sampling errors, or age and cause of death of the patient. With regard to age, it was recently reported that beta cells in old mice proliferate to a lesser degree than in young mice [9]. Indeed, when we repeated some of our measurements on 6- to 9-month-old mice, we found less beta cell proliferation than in mice aged 10 to 13 weeks (data not shown), supporting the above point.

In summary, we are the first to report on a coordinated peak of mRNA expression related to cell cycle genes in islets at day 9.5 of pregnancy. This diagnostic time course contrasted with most other differentially expressed genes unrelated to the cell cycle and allowed us to screen among poorly characterised genes for novel players in cell replication like *Fignl1* and *G7e*.

Acknowledgements We thank N. Buelens for her technical assistance in immunohistochemistry. We also thank S. Leach for help with Cytoscape analysis. MIN6 cells were kindly donated by E. Yamato (Division of Stem Cell Regulation Research, Osaka University Graduate School of Medicine, Osaka, Japan). This work was financially supported by grants from the European Community (EURODIA FP6-518153), the Juvenile Diabetes Research Foundation (JDRF 1-2010-393), the Belgian Ministry for Science Policy (IUAP P6/40) and the Katholieke Universiteit Leuven (SymBioSys and GOA 2008/16).

Duality of interest The authors declare that there is no duality of interest associated with this manuscript.

References

1. Butler PC, Meier JJ, Butler AE, Bhushan A (2007) The replication of beta cells in normal physiology, in disease and for therapy. Nat Clin Pract Endocrinol Metab 3:758–768
2. Heit JJ, Karnik SK, Kim SK (2006) Intrinsic regulators of pancreatic beta cell proliferation. Annu Rev Cell Dev Biol 22:311–338
3. Cozar-Castellano I, Fiaschi-Taesch N, Bigatel TA et al (2006) Molecular control of cell cycle progression in the pancreatic beta cell. Endocr Rev 27:356–370
4. Schwitzgebel VM, Somm E, Klee P (2009) Modeling intrauterine growth retardation in rodents: impact on pancreas development and glucose homeostasis. Mol Cell Endocrinol 304:78–83
5. Dhawan S, Georgia S, Bhushan A (2007) Formation and regeneration of the endocrine pancreas. Curr Opin Cell Biol 19:634–645
6. Bruning JC, Winnay J, Bonner-Weir S, Taylor SI, Accili D, Kahn CR (1997) Development of a novel polygenic model of NIDDM in mice heterozygous for IR and IRS-1 null alleles. Cell 88:561–572
7. Butler AE, Janson J, Bonner-Weir S, Ritzel R, Rizza RA, Butler PC (2003) Beta cell deficit and increased beta cell apoptosis in humans with type 2 diabetes. Diabetes 52:102–110
8. Cozar-Castellano I, Harb G, Selk K et al (2008) Lessons from the first comprehensive molecular characterization of cell cycle control in rodent insulinoma cell lines. Diabetes 57:3056–3068
9. Tschen SI, Dhawan S, Gurlo T, Bhushan A (2009) Age-dependent decline in beta cell proliferation restricts the capacity of beta cell regeneration in mice. Diabetes 58:1312–1320
10. Rieck S, Kaestner KH (2009) Expansion of beta cell mass in response to pregnancy. Trends Endocrinol Metab 21:151–158
11. Sorenson RL, Brelje TC (2009) Prolactin receptors are critical to the adaptation of islets to pregnancy. Endocrinology 150:1566–1569
12. Parsons JA, Brelje TC, Sorenson RL (1992) Adaptation of islets of Langerhans to pregnancy: increased islet cell proliferation and insulin secretion correlates with the onset of placental lactogen secretion. Endocrinology 130:1459–1466
13. Sorenson RL, Brelje TC (1997) Adaptation of islets of Langerhans to pregnancy: beta cell growth, enhanced insulin secretion and the role of lactogenic hormones. Horm Metab Res 29:301–307
14. Nadal A, Alonso-Magdalena P, Soriano S, Ropero AB, Quesada I (2009) The role of oestrogens in the adaptation of islets to insulin resistance. J Physiol 587:5031–5037
15. Huang C, Snider F, Cross JC (2009) Prolactin receptor is required for normal glucose homeostasis and modulation of beta cell mass during pregnancy. Endocrinology 150:1618–1626
16. Karnik SK, Chen H, McLean GW et al (2007) Menin controls growth of pancreatic beta cells in pregnant mice and promotes gestational diabetes mellitus. Science 318:806–809
17. Dreijerink KM, Hoppener JW, Timmers HM, Lips CJ (2006) Mechanisms of disease: multiple endocrine neoplasia type 1-relation to chromatin modifications and transcription regulation. Nat Clin Pract Endocrinol Metab 2:562–570
18. Zhang H, Zhang J, Pope CF et al (2010) Gestational diabetes mellitus resulting from impaired beta cell compensation in the absence of FoxM1, a novel downstream effector of placental lactogen. Diabetes 59:143–152
19. Zhang H, Ackermann AM, Gusarova GA et al (2006) The FoxM1 transcription factor is required to maintain pancreatic beta cell mass. Mol Endocrinol 20:1853–1866
20. Bernardo AS, Hay CW, Docherty K (2008) Pancreatic transcription factors and their role in the birth, life and survival of the pancreatic beta cell. Mol Cell Endocrinol 294:1–9

21. Ackermann MA, Costa RH, Gannon M (2008) Beta cell proliferation, but not neogenesis, following 60% partial pancreatectomy is impaired in the absence of FoxM1. Diabetes 57:3069–3077
22. Rieck S, White P, Schug J et al (2009) The transcriptional response of the islet to pregnancy in mice. Mol Endocrinol 23:1702–1712
23. Lemaire K, Ravier MA, Schraenen A et al (2009) Insulin crystallization depends on zinc transporter ZnT8 expression, but is not required for normal glucose homeostasis in mice. Proc Natl Acad Sci U S A 106:14872–14877
24. Thorrez L, Van Deun K, Tranchevent LC et al (2008) Using ribosomal protein genes as reference: a tale of caution. PLoS One 3:e1854
25. Jensen LJ, Kuhn M, Stark M et al (2009) STRING 8—a global view on proteins and their functional interactions in 630 organisms. Nucleic Acids Res 37:D412–D416
26. In't Veld P, Lievens D, De Grijse J et al (2007) Screening for insulitis in adult autoantibody-positive organ donors. Diabetes 56:2400–2404
27. Junttila MR, Puustinen P, Niemela M et al (2007) CIP2A inhibits PP2A in human malignancies. Cell 130:51–62
28. Hosokawa M, Takehara A, Matsuda K et al (2007) Oncogenic role of KIAA0101 interacting with proliferating cell nuclear antigen in pancreatic cancer. Cancer Res 67:2568–2576
29. Luke-Glaser S, Pintard L, Tyers M, Peter M (2007) The AAA-ATPase FIGL-1 controls mitotic progression, and its levels are regulated by the CUL-3MEL-26 E3 ligase in the C. elegans germ line. J Cell Sci 120:3179–3187
30. Park SJ, Kim SJ, Rhee Y et al (2007) Fidgetin-like 1 gene inhibited by basic fibroblast growth factor regulates the proliferation and differentiation of osteoblasts. J Bone Miner Res 22:889–896
31. Snoek M, Albertella MR, van Kooij M et al (2000) G7c, a novel gene in the mouse and human major histocompatibility complex class III region, possibly controlling lung tumor susceptibility. Immunogenetics 51:383–386
32. van Kooij M, de Groot K, van Vugt H, Aten J, Snoek M (2001) Genotype vs phenotype: conflicting results in mapping a lung tumor susceptibility locus to the G7c recombination interval in the mouse MHC class III region. Immunogenetics 53:656–661
33. Adler P, Kolde R, Kull M et al (2009) Mining for coexpression across hundreds of datasets using novel rank aggregation and visualization methods. Genome Biol 10:R139
34. Rhodes DR, Kalyana-Sundaram S, Mahavisno V et al (2007) Oncomine 3.0: genes, pathways, and networks in a collection of 18,000 cancer gene expression profiles. Neoplasia 9:166–180
35. Lyons BA, Parich RC (1994) Determination of lymphocyte division by flow cytometry. J Immunol Methods 171:131–137
36. Besson A, Dowdy SF, Roberts JM (2008) CDK inhibitors: cell cycle regulators and beyond. Dev Cell 14:159–169
37. Coqueret O (2003) New roles for p21 and p27 cell-cycle inhibitors: a function for each cell compartment? Trends Cell Biol 13:65–70
38. Groszer M, Erickson R, Scripture-Adams DD et al (2006) PTEN negatively regulates neural stem cell self-renewal by modulating G0-G1 cell cycle entry. Proc Natl Acad Sci U S A 103:111–116
39. Fujita Y, Hayashi T, Kiyomitsu T et al (2007) Priming of centromere for CENP-A recruitment by human hMis18alpha, hMis18beta, and M18BP1. Dev Cell 12:17–30
40. Turchi L, Fareh M, Aberdam E et al (2009) ATF3 and p15PAF are novel gatekeepers of genomic integrity upon UV stress. Cell Death Differ 16:728–737
41. Yamaguchi T, Cubizolles F, Zhang Y et al (2010) Histone deacetylases 1 and 2 act in concert to promote the G1-to-S progression. Genes Dev 24:455–469
42. Salazar G, Liu D, Liao C et al (2003) Apoptosis in male germ cells in response to cyclin A1-deficiency and cell cycle arrest. Biochem Pharmacol 66:1571–1579
43. Blangy A, Lane HA, d'Herin P, Harper M, Kress M, Nigg EA (1995) Phosphorylation by p34cdc2 regulates spindle association of human Eg5, a kinesin-related motor essential for bipolar spindle formation in vivo. Cell 83:1159–1169
44. Chauviere M, Kress C, Kress M (2008) Disruption of the mitotic kinesin Eg5 gene (Knsl1) results in early embryonic lethality. Biochem Biophys Res Commun 372:513–519
45. Valentine MT, Fordyce PM, Block SM (2006) Eg5 steps it up! Cell Div 1:31
46. Zhang Y, Xu W (2008) Progress on kinesin spindle protein inhibitors as anti-cancer agents. Anticancer Agents Med Chem 8:698–704
47. Sladek R, Rocheleau G, Rung J et al (2007) A genome-wide association study identifies novel risk loci for type 2 diabetes. Nature 445:881–885
48. Schraenen A, Lemaire K, de Faudeur G et al (2010) Placental lactogens induce serotonin biosynthesis in a subset of mouse beta cells during pregnancy. Diabetologia. doi:10.1007/s00125-010-1913-7
49. Van Assche FA, Aerts L, De Prins F (1978) A morphological study of the endocrine pancreas in human pregnancy. Br J Obstet Gynaecol 85:818–820
50. Butler AE, Cao-Minh L, Galasso R et al (2010) Adaptive changes in pancreatic beta cell fractional area and beta cell turnover in human pregnancy. Diabetologia 53:2167–2176